Spatio-temporal clustering of earthquakes: Comparative analysis of marginal vs. coupled components in different regions

Natalie Bladis and Ilya Zaliapin

University of Nevada, Reno, Department of Mathematics and Statistics

Abstract

Earthquake clustering is a fundamental component of seismicity that reflects various forms of earthquake triggering mechanisms. Zaliapin and Ben-Zion (SRL, 2021) introduced a simple and robust measure of space-time clustering, using the receiver operating characteristic (ROC) diagram, that allows disentangling effects related to concentration of events around a heterogeneous regional fault network (marginal space distribution of events) from coupled space-time fluctuations (joint space-time distribution). This work

- applies the clustering measure of Zaliapin and Ben-Zion (SRL, 2021) to examine additional regions (see **Data**)
- extends the analysis to a more general measure of seismic rate that can account for the number of events, the total area of faultbreaks, seismic moment, Benioff strain, etc. (see **Methodology**)
- systematically examines general and coupled space-time clustering of raw and declustered catalogs

Introduction/Background

A basic characteristic of seismicity is earthquake clustering. Clustering is observed most clearly as the concentration and frequency of earthquakes around large faults and tectonic plate boundaries (spatial clustering; see **Fig. 1**) and after large earthquakes (aftershocks). Other types of linked events, like foreshocks and swarms, are also connected to earthquake clustering. Understanding seismic clustering plays an important role in many elements of seismicity, such as identifying the characteristics and interactions of active fault structures. Using declustered catalogs (catalogs that do not include foreshocks, aftershocks and other strong forms of clustering) can uncover more subtle features of earthquake attributes and patterns. This poster is meant to illustrate and quantify earthquake clustering with examples of seismicity from southern California and other regions using the simple and robust measure of space-time clustering (see **Methodology**).

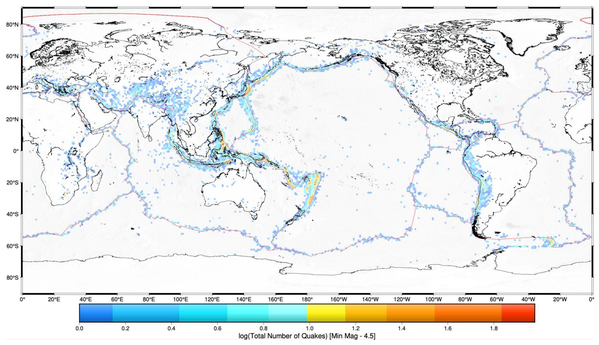

Figure 1: Clustering of global seismicity based on the ComCat catalog during the period of 1981–2022. Shades of color reflect the number of earthquakes (logarithmic scale; see color bar) with M ≥ 4.5 in square spatial cells with side length equal to 1°. Notice a significant space inhomogeneity.

Data

For this study, the ANSS Comprehensive Earthquake Catalog (ComCat) was used to examine seismicity in southern California, Japan, New Zealand and Italy. A summary of the parameters for the clustering analysis is displayed in **Table 1**.

Table 1 – Parameters of Catalog Analysis

Catalog	Space Range	Time Range	Magnitude Range	Number of Events	Size of Space Resolution, Δ (°)	Size of Temporal Resolution, w (years)	Threshold Σ_0
ComCat SoCal	124°-114°W; 30°-38°N	1971- 2022	2.3-7.3	113,290	0.6	1.5	0
ComCat Japan	128°-146°E; 30°- 47°N	1971- 2022	4.5-9.1	15,754	1	5	0
ComCat New Zealand	160°-180°E; 50°-30°S	1990-2022	4.4-7.8	3,153	1	6	0
ComCat Italy	0°-25°E; 30°-50°N	1983-2005	3.3-6	4,811	1	6	0

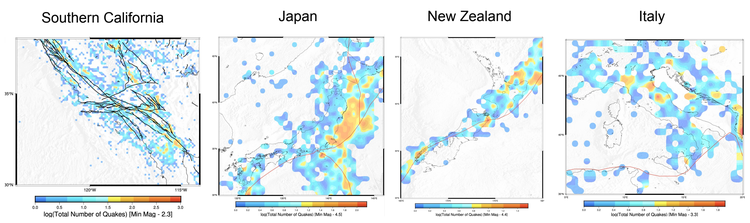

Figure 2: Regions examined for this study include southern California, Japan, New Zealand, and Italy. Shades of color reflect the number of events (logarithmic scale; see color bar) in each square spatial cell with the side length equal to 0.1° for Southern California and 0.5° for all other regions.

Methodology

Receiver operating characteristic (ROC) diagrams were used to assess the inhomogeneity of the space-time distribution of seismicity in the regions of this study in a systematic way. These ROC diagrams were used to produce a single measure of space-time clustering, the Gini coefficient (G) which is an efficient and stable measurement of earthquake clustering. The coefficient G may assume values between 0 and 1. A value of G close to 1 indicates a large portion of events are concentrated in a small fraction of the examined space-time volume.

More formally, we partition the examined space-time area into voxels with space dimension Δ and time size w, and measure seismic activity within a voxel centered at location $\mathbf{x}$ at time t by $\boldsymbol{\Sigma}(\mathbf{x},t) = \Sigma 10^{\beta M_i}$, where the summation is taken over all events within the voxel, β is a parameter, and M is the event magnitude. Notice that $\beta = 0$ corresponds to counting events, $\beta = 1$ approximates the faultbreak area, and $\beta = 3/2$ corresponds to the seismic moment. We only examine voxels with the time-integrated value of $\boldsymbol{\Sigma}$ being larger than a threshold $\boldsymbol{\Sigma}_0$ (in this work, $\boldsymbol{\Sigma}_0 = 0$).

First, we evaluate the general clustering. Here, the ROC diagram is a plot of $\boldsymbol{\Sigma}$ within the most active voxels (y-axis) vs. the fraction of the examined non-empty voxels (x-axis); see Fig. 3. Next, in order to remove the effects of marginal space and time heterogeneities in the examined catalog, we evaluate coupled space-time clustering. In this analysis, the ROC diagram is a plot of $\boldsymbol{\Sigma}$ within the most active voxels (y-axis) vs. the weighted fraction of the examined non-empty voxels. The weights are determined by the factorized space-time rates of background events: $J(\mathbf{x},t) = S(\mathbf{x})xT(t)$, where $S(\mathbf{x})$ is the marginal space rate of the background events (that reflects regional space heterogeneities related to the fault network), and $T(t)$ is the marginal time rate of events (that reflects possible marginal temporal heterogeneities, which are negligible in most of the examined cases). Declustering is done by the method of Zaliapin and Ben-Zion (JGR, 2020)

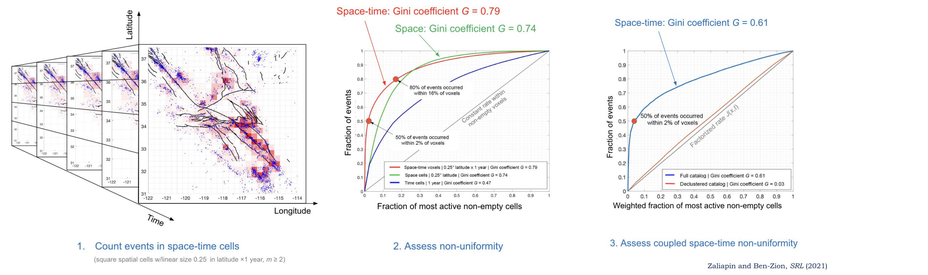

Figure 3: Quantifying clustering of earthquakes in southern California with the receiver operating characteristic (ROC) diagram. The analysis uses the catalog of Hauksson et al. (2012, extended) during 1981–2020 with magnitude M ≥ 2, and space– time voxels with square space projection of latitude size 0.25° and 1 yr duration.

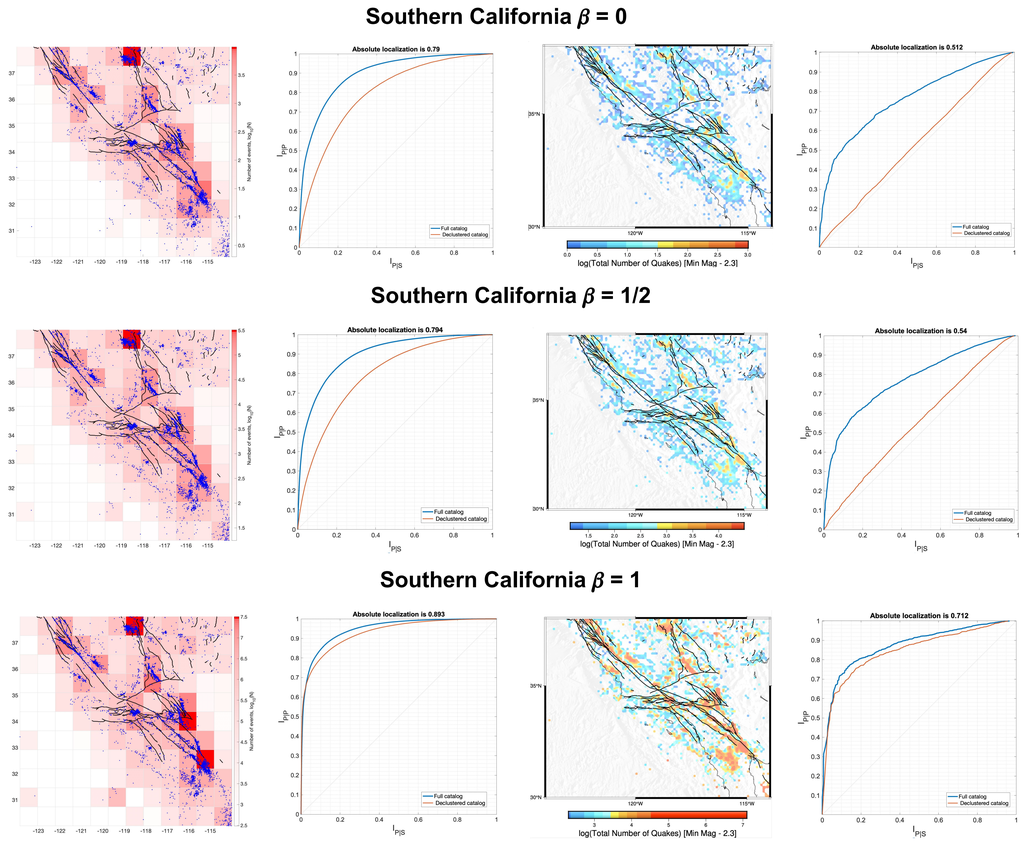

Figure 4: Analysis of earthquake clustering in Southern California. The first plot for each β value shows the location of earthquakes larger than magnitude 3.5 as blue dots. The red shaded regions show the total number of events (on a log scale, see color bar) in each spatial cell with side length equal to 0.6°. The second plot for each β value shows the localization results with respect to a uniform measure for the full catalog (blue line) and declustered catalog (red line). The third plot illustrates the $\boldsymbol{\Sigma}$ value in each square spatial cell with the side length equal to 0.1°. The fourth plot for each β value shows the localization results with respect to a factorized measure $J(\mathbf{x},t)$ for the full catalog (blue line) and declustered catalog (red line).

Results

Table 2 – Localization Results (Beta = 0)

Catalog	Clustering with Respect to Constant Rate, G	Background Clustering with Respect to Constant Rate, G	Clustering with Respect to Factorized Rate, G	Background Clustering with Respect to Factorized Rate, G
ComCat SoCal	0.79	0.53	0.55	0.07
ComCat Japan	0.71	0.57	0.35	0.06
ComCat New Zealand	0.62	0.47	0.35	0.08
ComCat Italy	0.64	0.50	0.28	0.03

Table 3 – Localization Results (Beta = 1/2)

Catalog	Clustering with Respect to Constant Rate, G	Background Clustering with Respect to Constant Rate, G	Clustering with Respect to Factorized Rate, G	Background Clustering with Respect to Factorized Rate, G
ComCat SoCal	0.80	0.55	0.57	0.14
ComCat Japan	0.71	0.58	0.36	0.08
ComCat New Zealand	0.64	0.51	0.38	0.15
ComCat Italy	0.65	0.51	0.30	0.06

Table 4 – Localization Results (Beta = 1)

Catalog	Clustering with Respect to Constant Rate, G	Background Clustering with Respect to Constant Rate, G	Clustering with Respect to Factorized Rate, G	Background Clustering with Respect to Factorized Rate, G
ComCat SoCal	0.91	0.86	0.75	0.70
ComCat Japan	0.87	0.77	0.64	0.44
ComCat New Zealand	0.80	0.83	0.55	0.61
ComCat Italy	0.73	0.66	0.40	0.24

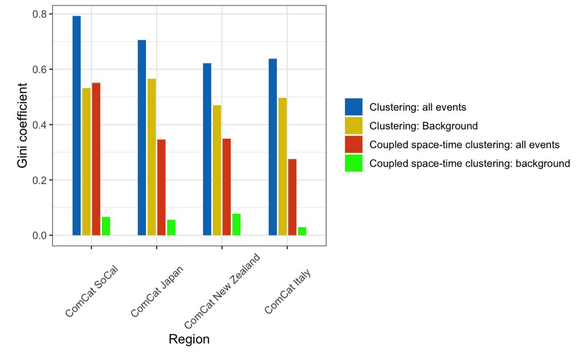

Figure 5: Quantifying earthquake clustering. Summary of results for all regions for $\beta = 0$.

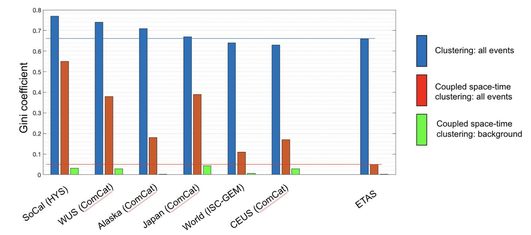

Figure 6: Past results quantifying earthquake clustering for $\beta = 0$ in several regions and ETAS model (Zaliapin and Ben-Zion, SRL, 2021). The results are similar to results of this study.

Summary/Conclusions

- The overall observed earthquake clustering is high, both for raw catalog (G > 0.6) and declustered catalog (G > 0.4)
- The marginal space clustering (fault network) plays a dominant role in the overall clustering
- When focusing on the coupled space-time clustering, different catalogs show different degrees of clustering (0.1 < G < 0.6), reflecting a variety of specific triggering conditions and mechanisms
- Coupled clustering of declustered catalogs (for $\beta = 0$) is negligible (G < 0.1)

References

1. Zaliapin, I. and Y. Ben-Zion (2021) Perspectives on clustering and declustering of earthquakes. *Seismological Research Letters*, 93 (1): 386–401 doi:10.1785/0220210127
2. Zaliapin, I. and Y. Ben-Zion (2020) Earthquake declustering using the nearest-neighbor approach in space-time-magnitude domain. *J. Geophys. Res.: Solid Earth*, e53991, doi:10.1029/2018JB017120

Acknowledgements

The study was supported by the National Science Foundation (grant EAR-2122191) and the Southern California Earthquake Center project 22090.